

Characterization of short fiber-reinforced polylactic acid composites produced with
Fused Filament Fabrication (FFF)

Tóth Cs., Kovács N. K.

Accepted for publication in IOP Conference Series: Materials Science and
Engineering

Published in -0001

DOI:

PAPER • OPEN ACCESS

Characterization of short fiber-reinforced polylactic acid composites produced with Fused Filament Fabrication (FFF)

To cite this article: Tóth Csenge and Krisztián Norbert Kovács 2020 *IOP Conf. Ser.: Mater. Sci. Eng.* **903** 012031

View the [article online](#) for updates and enhancements.



The banner features a background image of Earth from space. On the left, there are three circular logos: the top one is 'ECS' in a circle, the middle one is 'The Electrochemical Society' with a stylized 'ECS' logo, and the bottom one is 'THE KOREAN ELECTROCHEMICAL SOCIETY'. The main text in the center reads 'Joint International Meeting PRiME 2020 October 4-9, 2020'. Below this, a blue bar contains the text 'Attendees register at NO COST!'. On the right side, there is a large 'PRIME' logo with 'PACIFIC RIM MEETING ON ELECTROCHEMICAL AND SOLID STATE SCIENCE' underneath, and '2020' in large numbers. At the bottom right, a blue bar contains the text 'REGISTER NOW' with a right-pointing arrow.

Characterization of short fiber-reinforced polylactic acid composites produced with Fused Filament Fabrication (FFF)

Csenge Tóth and Krisztián Norbert Kovács

Department of Polymer Engineering, Faculty of Mechanical Engineering, Budapest University of Technology and Economics, H-1111 Budapest, Műegyetem rkp. 3., Hungary

E-mail: kovacs@pt.bme.hu

Abstract. The interdisciplinary expansion of additive manufacturing (AM) technologies resulted in an increasing demand for high-performance materials for engineering applications. In order to enhance the mechanical properties of printed products, short fiber composites are of great interest recently. In this study, the development of short fiber-reinforced composite materials is performed along with the mechanical characterization of the samples produced by fused filament fabrication (FFF) technology.

1. Introduction

Fused filament fabrication (FFF) is one of the most popular AM technologies due to its cost efficiency and low waste production, and as the technology attracted attention in various industries, the demand for high-performance materials rose as well. A commonly used material for FFF technology is polylactic acid (PLA) due to its good printing properties, and as a result of the recent increasing interest in sustainable solutions, PLA became a desirable alternative to oil-based polymers. While the good tensile strength (60 MPa) and competitive price (2 Euro/kg) make PLA a standout among biopolymers, it still has some disadvantages that need to be addressed [1,2].

A way to improve the mechanical properties of printed PLA products is the optimization of manufacturing parameters such as the build orientation, feed rate, and layer thickness [3], however, these technology-dependent solutions might not be applicable for all geometries. Another way to enhance the mechanical properties of PLA is the use of blends. For instance, Hajba et al [4] reported that toughness can be improved with natural rubber particles. Fiber reinforcement could also be a viable solution especially in case of FFF technology since short fiber filaments can be processed with most any FFF printer, although the fiber content is reported to be limited to 30 w% [5,6]. In addition to the limitation in fiber content, short fibers seem to bring several further challenges. First, selecting the most suitable fiber type for PLA is essential as it affects the overall mechanical properties greatly. Sang et al [7] reported that basalt fiber composites showed better tensile and flexural properties compared to carbon fiber PLA composites due to rheological differences. Ferreira et al [8] also found the tensile strength of PLA/CF composites to be unsatisfactory which was caused by poor fiber-matrix adhesion.

Reaching the critical fiber length is also a challenging task for short fiber FFF technology, as the shear stress of the filament manufacturing process results in fiber breakage [9]. Moreover, the increase of fiber content results in further fiber breakage as more fiber-fiber interactions are present [6]. However, a promising feature of the FFF composite technology is the fiber orientation. It is demonstrated in studies



that during printing, a highly oriented material is gained due to the small diameter of the nozzle and the draw speed [6,10]. Since the orientation is parallel to the printing direction, it is feasible to produce composite parts with unique reinforcement patterns with FFF technology. This aspect of the technology could be beneficial in producing final parts and additionally, FFF printing has a good potential in complementing other thermoplastic manufacturing technologies as well [11]. The strength of the technology lies in its design freedom since the production of complex geometries with traditional composite technologies could face numerous challenges [12]. Also, the high degree of automation of AM technologies makes it ideal for integration into industry 4.0 systems as well.

To the best of our knowledge, most of the studies investigated short carbon fiber reinforced materials regarding FFF processes, therefore this paper aims to expand the range of materials. In addition to carbon and glass fibers, basalt fibers are also investigated. Their excellent mechanical properties and the lower energy consumption during production can make basalt fibers a favourable alternative to glass fibers [7,13]. The printing orientation is also considered in this study, for which samples were made with two types of printing orientation. Mechanical tests were carried out as well as optical experiments to gain knowledge on the adhesion conditions and the degree of fiber fracturing during FFF technology.

2. Experimental methods

2.1. Raw materials

The PLA (Ingeo 3100HP, Melt Flow Rate 24 g/10 min (210 °C/2,16 kg)) used in this study as matrix material was obtained from NatureWorks. The self-made composite filaments contained chopped Zoltek PX35 carbon fibers (CF), Camelyaf glass fibers (GF), and Kamenny vek basalt fibers (BF) respectively. The average fiber length is 6 mm. Mixtures of 5 weight % fiber content were prepared for each and a neat 3100HP PLA filament was made for control. The commercially available Proto-Pasta PLA/15 w% CF composite filament was also examined and the unfilled PLA (NatureWorks Ingeo 4043D, Melt Flow Rate 6 g/10 min (210 °C/2,16 kg)) material was used as a reference. All composite filaments are summarized in table 1.

2.2. Preparation of composite filaments

First, the mixtures were fed to a twin-screw extruder (Labtech LTE 26-44) in a dry state (80 °C/4h). Preforms were made and granulated of 6 mm length, then extruded again using a cylindrical die. The two-step manufacturing process was necessary as the first extrusion resulted in an uneven filament diameter, which led to irregular material flow during printing.

Table 1. Composite filaments.

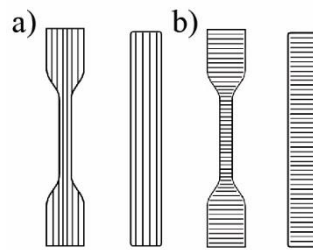
Matrix	Reinforcement	Weight fraction (weight %)	Manufacturer
3100HP PLA	BF	5	self-made
	CF	5	self-made
	GF	5	self-made
4043D PLA	CF	15	Proto-Pasta

2.3. 3D printing

Samples were prepared by a desktop FFF printer (CraftBot Plus). Table 2. show the process parameters. The intention was to maintain the same process parameters for each material, however, the extrusion of the 15 w% CF composite filament required a higher nozzle temperature as the flowability of the material decreased by the rigid carbon fibers [7]. The samples were fabricated with two types of unidirectional printing orientations (see figure 1.) and the infill was set to 100%. One contour layer of 0,4 mm was applied.

Table 2. Printing parameters.

Nozzle temperature 5 w% (°C)	215
Nozzle temperature 15 w% (°C)	230
Bed temperature (°C)	60
Nozzle diameter (mm)	0,4
Speed (mm/s)	60
Infill (%)	100
Layer height (mm)	0,2

**Figure 1.** Printing orientations of the specimens: a) parallel (0°) and b) perpendicular to the length (90°).

2.4. Mechanical properties

Tensile tests were conducted on a Zwick Z005 testing equipment according to the ISO 527-2 [14] standard, with a crosshead speed of 5 mm/min. Flexural properties were determined by 3-point bending tests in accordance with the ISO 178 [15] standard. During these experiments, 5 specimens per type were examined. Finally, impact strength was measured on notched specimens using a Charpy impact machine (Ceast Resil Impactor Junior equipped with a pendulum of 2 J) according to the ISO 179 [16] standard. Notch radius was $0,25 \pm 0,05$ mm. 10 specimens per type were used to measure the impact strength. All tests were performed at room temperature.

Fiber length distributions were measured to determine the extent of fiber breakage during the material extrusion and FFF printing. For this purpose, samples were obtained from the composite filaments and the FFF processed materials both, then the samples were heated up to 500 °C for 3 hours to remove the PLA matrix. Heating was conducted in a laboratory furnace under air atmosphere (type Denkal 6B). The extracted fibers were transferred onto glass plates, then the images of the fibers were taken with a Keyence VHX 5000 digital microscope. Fiber length distributions were obtained from the pictures using ImageJ software and about 200 fibers were measured each.

SEM micrographs of cryogenic fracture surfaces were taken with a JEOL JSM 6380LA equipment at an acceleration voltage of 10 kV. The surfaces of the samples were gold plated in vacuum. The internal morphology was also observed via non-destructive micro-computed tomography (Nikon XT H 225 ST). The sample for the μ -CT analysis was prepared with 0° printing orientation with 80 x 10 x 4 mm dimensions. The high-resolution technique resulted in a complete 3D visualization of the composite specimen.

3. Results and discussion

3.1. Fiber length distribution

The fiber length distribution (FLD) in the composite filaments and the FFF processed materials are shown in figure 2. All filaments were extruded twice, and all materials have the same initial fiber length of 6 mm. Significant fiber breakage occurred during the filament extrusion due to the high shear forces generated by the twin-screw extruder. However, it can be stated that the FFF process causes further fiber breakage only to a slight extent. The carbon and glass fibers longer than 300-400 μ m decreased more while the basalt fibers showed no significant change in the FLDs. In summary, all fiber types followed a similar trend, and the material extrusion through the nozzle during FFF printing did not alter the average fiber lengths drastically.

Theoretical critical fiber lengths for polylactic matrix and basalt, carbon, and glass fibers were calculated based on literature data [17,18,19] and this resulted in the ranges of 600-1000 μ m, 1000-1200 μ m and 800-1200 μ m, respectively. For carbon and glass fibers this theoretical length is yet to be achieved, however, the FLD of the basalt fibers shows a promising amount of fibers in the desired range. The remaining fiber lengths could be improved by applying a gentler extrusion process, or the theoretical critical fiber length could be decreased by optimizing the fiber-matrix adhesion thus increasing the interfacial shear strength.

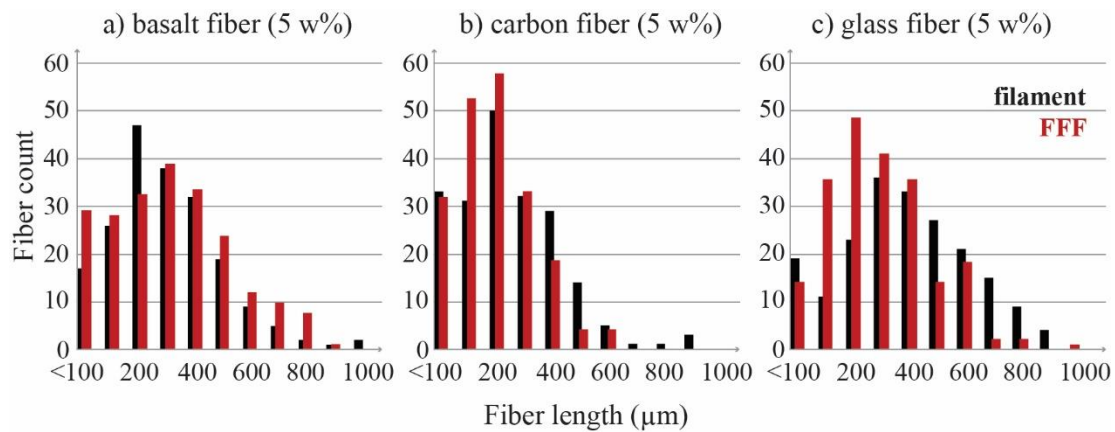


Figure 2. Fiber length distributions obtained from filaments and FFF processed materials: a) PLA/5 w% BF, b) PLA/5 w% CF, c) PLA/5 w% GF.

3.2. Mechanical characterization

In the following chapters, the mechanical properties are presented as percentage deviations from the corresponding references. The values of the matrix materials are shown in Table 3.

Table 3. Reference materials.

Properties	3100HP 0°		3100HP 90°		4043D 0°		4043D 90°	
	Avg.	Dev.	Avg.	Dev.	Avg.	Dev.	Avg.	Dev.
Tensile strength (MPa)	45	1,33	41	1,30	52	2,88	49	2,16
Tensile modulus (GPa)	2,4	0,05	2,5	0,04	0,7	0,11	0,4	0,11
Flexural strength (MPa)	88	5,88	74	3,97	91	1,50	84	5,18
Flexural modulus (GPa)	2,4	0,14	2,3	0,06	2,4	0,04	2,2	0,23
Impact strength (kJ/m ²)	3,2	0,55	3,0	0,45	5,2	0,89	3,6	0,48

3.2.1. Tensile properties. The effects of the printing orientation and the different types of fiber reinforcements on the tensile strength and Young's modulus are shown in figure 3. and figure 4., respectively. An increase in tensile strength can be observed in all 5 w% samples where the printing direction is longitudinal (0°), however, among the 90° printed samples only the BF material showed a significant rise in strength. Contrary to expectation, the increased fiber content did not result in bigger tensile strengths (as the 0° printed 15 w% CF specimens showed less than 5% development), moreover, the strength of the 15 w% CF 90° samples decreased. Literature also states that PLA/CF composites tend to have a bigger dependency on infill orientation, which is caused by relatively weak interlayer adhesion [7, 20].

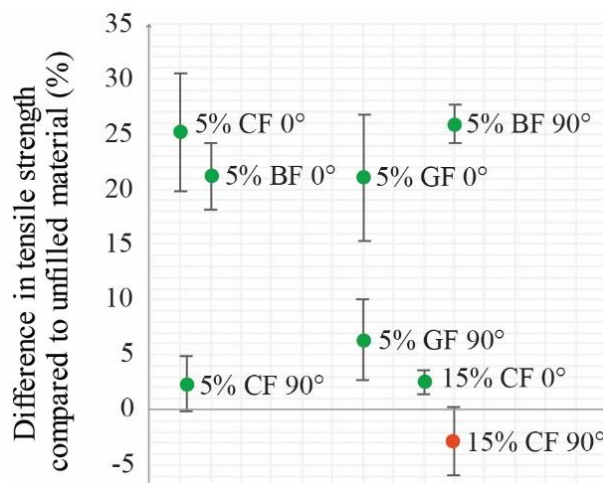


Figure 3. Percentage deviation of tensile strengths compared to the matrix PLA.

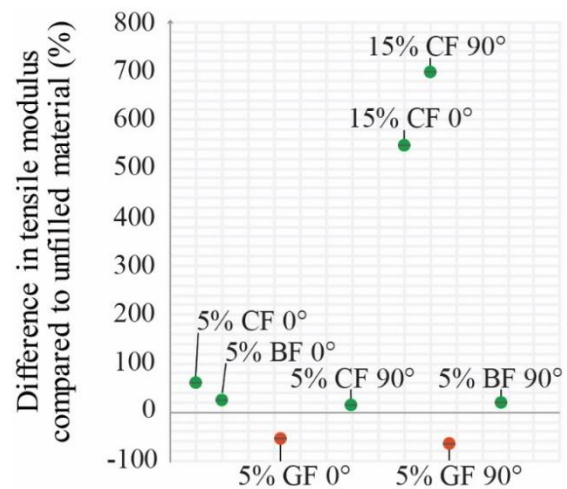


Figure 4. Percentage deviation of tensile moduli compared to the matrix PLA.

3.2.2. Flexural properties. A comparison of flexural properties (strength and modulus) between composites and neat materials are shown in figure 5. and figure 6. Only the glass fibers could improve the flexural strength, all the other types of reinforcements resulted in a decrease. On the other hand, the flexural modulus values mostly improved. In comparison with the tensile properties, it can be stated that the flexural properties have a bigger dependency on printing orientation.

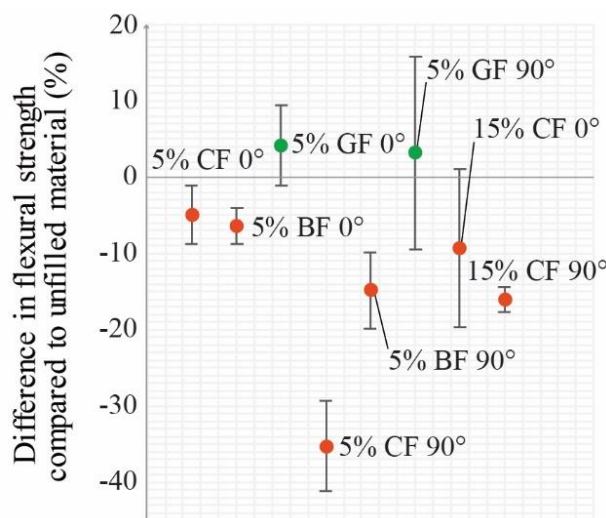


Figure 5. Percentage deviation of flexural strengths compared to the matrix PLA.

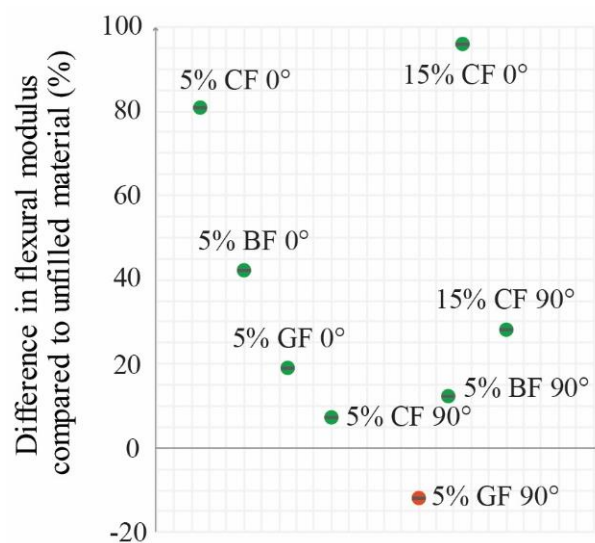


Figure 6. Percentage deviation of flexural moduli compared to the matrix PLA.

3.2.3. Impact strength and ductility. The effects of fibers and infill orientation on impact strength are shown in figure 7. It can be observed that the 5 w% and 15 w% fiber content mostly decreased the impact strengths, except for the 5 w% carbon and glass composites with parallel infill. The results presented may be due to low average fiber length or poor interfacial adhesion. Furthermore, it can be stated that with lower fiber content, it is statistically less likely for fibers to prevent crack propagation. figure 8. shows the differences in ductility between composites and neat plastic specimens. The ductility index decreased as fibers were added which means the composites became less rigid than the matrix PLA.

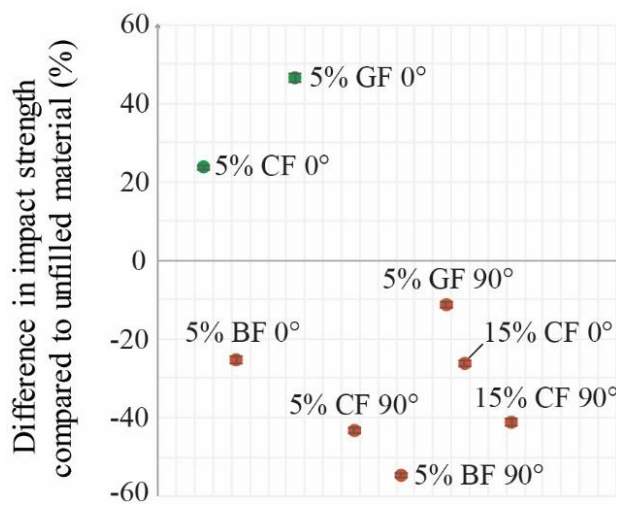


Figure 7. Percentage deviation of impact strengths compared to the matrix PLA.

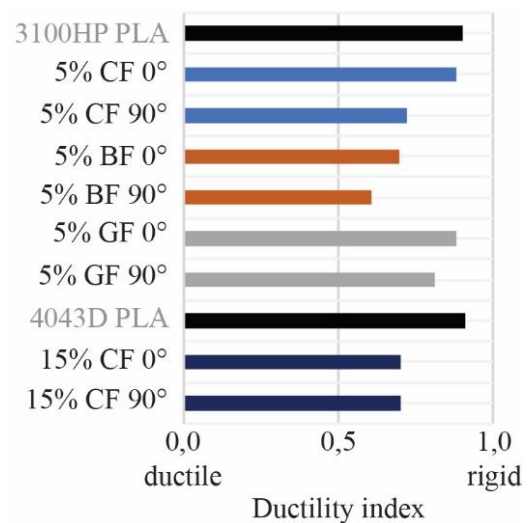


Figure 8. Ductility index of the composites and the unfilled PLA materials.

3.3. Microstructure

3.3.1. Void formation. SEM images of the cryogenic fracture surfaces of 5 w% basalt and carbon samples and 15 w% carbon sample are shown in figure 9. The printing orientation of the specimens is perpendicular to the fracture surface. Significant porosity can be observed on the 15 w% carbon sample made from the commercially available filament. The voids are of similar size and they are evenly dispersed through the surface. In contrast, the samples produced with self-made filaments show an unevenly dispersed porosity and the voids also differ in size. This is likely to be caused by the uneven diameter of the self-made filaments which potentially generates irregular material flow during printing. The pore formation can also be observed on the microtomographic images shown in figure 10. The complete 3D visualization confirmed that the samples present an all-over uneven nature in porosity which can be traced back to the fluctuating polymer flow.

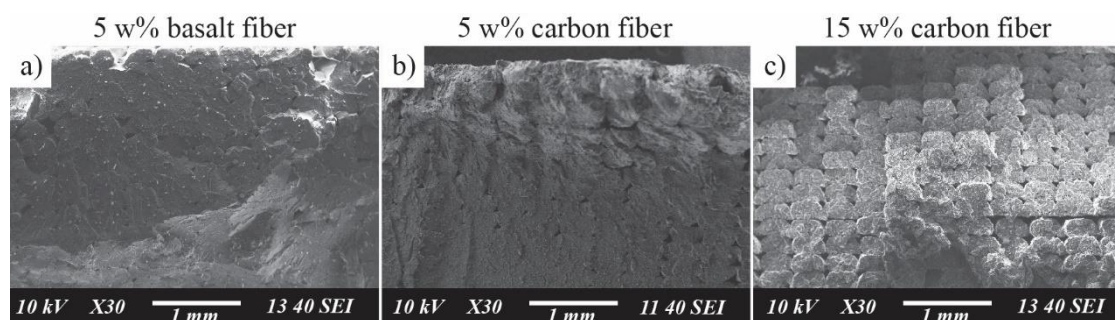


Figure 9. SEM images of cryogenic fracture surfaces of samples with 0° printing orientation: a) PLA/5 w% BF b) PLA/5 w% CF and c) PLA/15 w% CF specimens.

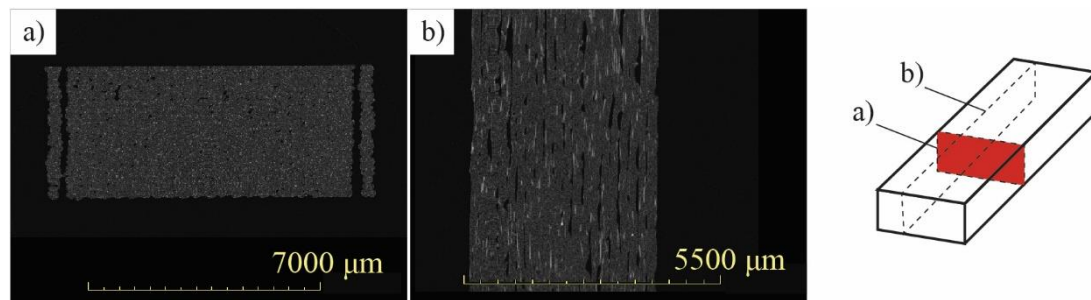


Figure 10. Microtomographic images of PLA/5 w% BF FFF printed sample with 0° printing orientation. Cross-sections shown are a) perpendicular and b) parallel to the printing direction.

3.3.2. Fiber orientation. Figure 11. shows the 3D microtomographic image of a basalt fiber-reinforced specimen with 5 w% fiber content. It can be observed that most of the fibers are oriented in the print direction in agreement with the literature [7]. The slight sinking of the upper layers can also be detected which is presumably caused by the relatively high degree of porosity underneath.

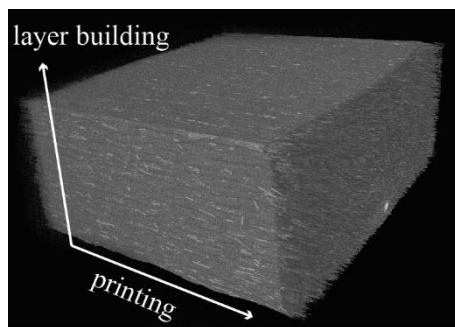


Figure 11. 3D microtomographic image of PLA/5 w% BF FDM printed sample with 0° printing orientation.

3.3.3. Fiber-matrix adhesion. SEM images of basalt and carbon fiber-reinforced samples are shown in figure 12. It can be seen that protruding carbon fibers are mostly clear from PLA, indicating poor fiber-matrix adhesion. On the other hand, the basalt fibers are covered with the matrix material to a moderately bigger extent. When examining the adhesion, it should be borne in mind that the basalt fibers were treated with a silane-based coupling agent, and it is recommended by the manufacturer for epoxy resin matrices. The surface treatment of carbon fibers used for the self-made filament is optimal for thermoplastic matrix materials.

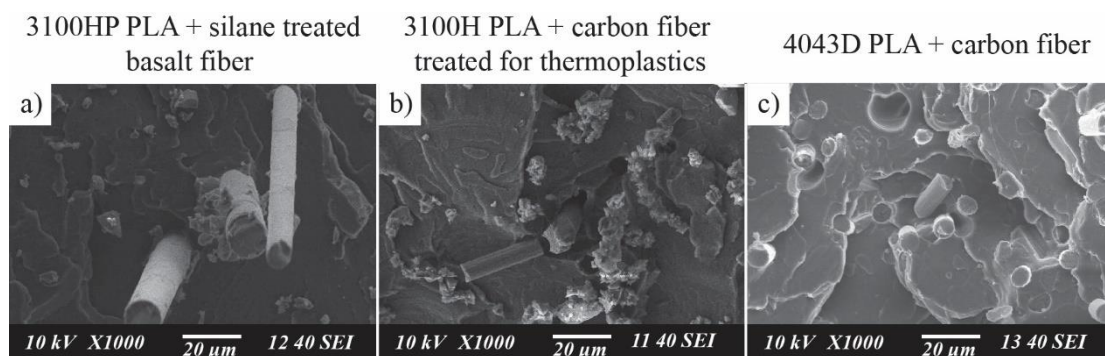


Figure 12. SEM images of FDM-printed samples: a) PLA/5 w% BF and b) PLA/5 w% CF are prepared with self-made composite filaments and c) PLA/15 w% CF is from commercially available material.

4. Conclusion

In this research, carbon, glass and basalt fiber-reinforced composite filaments are successfully fabricated and examined along with a commercially available PLA/CF filament. The fiber content is considered as the self-made composite filaments are prepared with 5 w% fiber content each and the PLA/CF material is loaded with 15 w% of fibers. Specimens were fabricated with FFF technology and two types of printing orientation were applied. Mechanical and optical characterizations were conducted and fiber

length distributions were measured to determine the extent of fiber breakage during the filament extrusion and the FFF process.

The results show that the average fiber length decreased significantly during the filament extrusion process due to high shear rates, however, the FFF printing does not cause further significant breakage. The 5 w% fiber content with the parallel infill resulted in an average of 20% increase in tensile strength values, but contrary to expectation, the 15 w% carbon fiber content resulted in a slight increase only. The flexural properties and the impact strengths of the composite materials showed no significant development compared to the unfilled matrices. Based on the results presented, the mechanical properties of the CF composites are the most dependent on the printing orientation. Scanning electron microscopy showed a better fiber-matrix adhesion for basalt fibers, which can be further improved by applying a more suitable surface treatment, specifically for the PLA matrix. Finally, microtomography showed a relatively high porosity in the specimens which is likely caused by irregular material flow during printing. The porosity might be reduced by increasing the feed rate or decreasing the draw speed.

With FFF technology it is possible to produce complex geometries with custom fiber orientation, therefore it could be an excellent alternative for thermoplastic composite manufacturing. However, further research and development are still necessary for engineers to be able to use the technology in its full potential. The results of this paper contribute to a deeper understanding of the relationships between processing parameters and mechanical properties. Optimization is required especially in terms of the fiber length, fiber-matrix adhesion, and porosity. Our further research focuses on basalt fiber-reinforced composites due to the good tensile properties and the favourable features of the basalt fibers.

Acknowledgments

The project is funded by the (NKFIH) National Research, Development and Innovation Office (2018 - 1.3.1 – VKE – 2018 - 00001).

This publication was supported by the Italian-Hungarian bilateral agreement of the CNR (Research National Council) and MTA (Hungarian Academy of Sciences).

References

- [1] Auras R et al 2001 *Poly(Lactic Acid): Synthesis, Structures, Properties, Processing, and Applications* (John Wiley&Sons Inc., Hoboken, New Jersey)
- [2] D Garlotta 2001 *Journal of Polymers and the Environment* **9(2)** 63-84
- [3] J M Chacón et al 2017 *Materials&Design* **124** 143-157
- [4] Hajba S and Tábi T 2019 *Periodica Polytechnica Ser. Mech. Eng.* **63(4)** 270-277
- [5] Hull et al 2015 *Proceedings of the ASME 2015 Int. Manuf. Sc. and Eng. Conference*
- [6] H L Tekinalp et al 2014 *Composites Science and Technology* **105** 144-150
- [7] L Sang et al 2019 *Composites Part B: Engineering* **164** 629-639
- [8] R T L Ferreira et al 2017 *Composites Part B* **124** 88-100
- [9] Dunai A and Macskási L 2003 *Műanyagok fröccsöntése* (Lexica Kft, Budapest)
- [10] X Wang et al 2017 *Composites Part B* **110** 442-458
- [11] Boros R et al 2019 *Express Polymer Letters* **13** 889-897
- [12] Geier N and Pereszlai Cs 2020 *Periodica Polytechnica Ser. Mech. Eng.* **64(1)** 67-80
- [13] Czigány T et al 2005 *Periodica Polytechnica Ser. Mech. Eng.* **49** 3-14
- [14] MSZ EN ISO 527: Plastics. Determination of tensile properties. (2012)
- [15] MSZ EN ISO 178: Plastics. Determination of flexural properties (2011)
- [16] MSZ EN ISO 179: Plastics. Determination of Charpy impact properties. (2010)
- [17] V Fiore et al 2015 *Composites Part B: Engineering* **74** 74-94
- [18] Y Z Wan et al 2001 *Journal of Applied Polymer Science* **82** 150-158
- [19] M J Mochane et al 2019 *Express Polymer Letters* **13** 159-198
- [20] S Yu 2019 *Composites Science and Technology* **175** 18-27